

# Orthogonalized Spatial Multiplexing for Closed-Loop MIMO Systems

Heunchul Lee, *Student Member, IEEE*, Seokhwan Park, *Student Member, IEEE*, and Inkyu Lee, *Senior Member, IEEE*

**Abstract**—In this paper, we propose a novel spatial multiplexing (SM) scheme for transmission over flat-fading multiple-input multiple-output (MIMO) channels, which allows simple maximum-likelihood decoding at the receiver with small feedback information. We begin with a real-valued representation of the complex-valued system model, and show that we can achieve orthogonality between transmitted signals by applying a proper rotation to transmitted symbols. Compared with other closed-loop methods, the proposed scheme significantly reduces the processing complexity at both transmitter and receiver as well as the feedback overhead. We also combine the proposed orthogonalization method with antenna-selection techniques, and then discuss a criterion based on the minimum Euclidean distance between received vectors for selecting the optimal subset of multiple transmit antennas. Using geometrical properties of the receive constellations, we also present a simple antenna-selection metric for the proposed SM systems. Simulation results demonstrate that our SM system performs close to the optimum closed-loop system with much-reduced complexity.

**Index Terms**—Closed-loop multiple-input multiple-output (MIMO) systems, maximum-likelihood decoding (MLD), spatial multiplexing (SM), transmit-antenna selection.

## I. INTRODUCTION

MULTIPLE-INPUT multiple-output (MIMO) systems provide a very promising means to increase the spectral efficiency for wireless systems. Especially, spatial multiplexing (SM) schemes enable extremely high spectral efficiencies by transmitting independent streams of data simultaneously through multiple transmit antennas [1]–[3]. Assuming perfect channel knowledge at the receiver, the potential gains of using the MIMO systems are well presented in [4] and [5].

In order to fully exploit the potential of multiple antennas and achieve the promised capacity, we can apply full channel state information (CSI) knowledge to the transmit side to optimize the transmission scheme according to current channel conditions. Based on knowledge of the full CSI at the transmitter, a basic idea of precoding has been proposed [6], [7]. The optimization of linear precoding and decoding has been presented

in [8] and [9]. Most work on these closed-loop MIMO systems is carried out by obtaining singular value decomposition (SVD) of the channel transfer matrix. It is well known that the optimum linear precoder and decoder decouple the MIMO channel into several independent eigensubchannels, and allocate resources such as power and bits over these subchannels.

More realistic assumptions about CSI at the transmitter and receiver can impact the potential channel gains of MIMO systems [10]–[12]. While CSI can be acquired at the transmitter by assuming channel reciprocity between uplink and downlink transmission in time-division duplex (TDD) systems, more often CSI needs to be obtained at the receiver and sent back to the transmitter over a reliable feedback channel [13]. However, in practical situations, the amount of feedback from the receiver to the transmitter should be kept as small as possible to minimize the overhead. In this sense, the assumption of full channel knowledge at the transmitter is not realistic, since even under flat-fading MIMO channels, the feedback requirements generally grow with the number of transmit antennas, receive antennas, and users. Another drawback of precoding systems is that the SVD operation requires high computational complexity and is known to be numerically sensitive [14].

To address these issues, the transmitter with limited feedback information in a communication system tries to use the system resources more efficiently [12], [13]. Precoding based on the limited feedback has been proposed in [15] and [16], where the transmit precoder is chosen from a finite set of precoding matrices, called codebook, known to both the receiver and transmitter. The receiver selects the optimal precoder from the codebook with a selection criterion based on the current CSI, and reports the index of this matrix to the transmitter over a limited feedback channel.

In this paper, we propose a new SM scheme for a closed-loop MIMO system which allows a simple maximum-likelihood (ML) receiver. Our interest is restricted to SM systems transmitting two independent data streams, which are important in practical wireless system designs. We first present a new orthogonal SM (OSM) scheme with reduced complexity and overhead. The ML decoding (MLD) is optimal for detecting symbols in MIMO SM systems. However, its computational complexity becomes exponential with the number of transmit antennas and the size of constellations. In order to reduce the processing complexity of an ML receiver, we propose a new SM system which requires only a single phase value from the receiver. To simplify the MLD, we first introduce a real-valued representation for complex-valued MIMO systems and propose a single-symbol decodable SM scheme based on the phase feedback. Transmitted signals from one transmit antenna are rotated by the phase value

Paper approved by D. L. Goeckel, the Editor for Wireless Communications of the IEEE Communications Society. Manuscript received December 26, 2005; revised May 1, 2006. This work was supported in part by the Ministry of Information and Communication (MIC), Korea, under the Information Technology Research Center (ITRC) support program, supervised by the Institute of Information Technology Assessment (IITA), and in part by Basic Research Program of the Korea Science and Engineering Foundation under Grant R01-2006-000-11112-0. This paper was presented in part at the IEEE Vehicular Technology Conference, Montreal, QC, Canada, September 2006.

The authors are with the School of Electrical Engineering, Korea University, Seoul 136-701, Korea (e-mail: heunchul@wireless.korea.ac.kr; shpark@wireless.korea.ac.kr; inkyu@korea.ac.kr).

Digital Object Identifier 10.1109/TCOMM.2007.894114

reported from the receiver. We will show a way of selecting appropriate rotation angles to obtain the orthogonality among transmitted symbols.

Next, we extend the proposed SM scheme to systems with a larger number of transmit antennas. When there are more than two transmit antennas, our proposed scheme needs to choose the two best antennas to maximize the performance. The transmit-antenna subset selection can be viewed as another example of limited feedback precoding, where the optimal subset of transmit antennas is determined and conveyed to the transmitter. Simultaneous transmission from all available transmit antennas may incur too much burden on system complexity due to the increased number of radio-frequency (RF) chains. To reduce the cost, a selection criterion based on the output signal-to-noise ratio (SNR) is proposed for SM systems with linear receivers in [17]. Various criteria for selecting the transmitter subset are derived in [18] and [19].

In this paper, we consider a criterion based on the minimum Euclidean distance for selecting the optimal subset of multiple transmit antennas in the proposed SM systems, since the Euclidean distance between received vectors accounts for the symbol-error probability [20]. Although the computation of the minimum Euclidean distance requires a full search over the multidimensional constellation in the conventional SM systems, we show that the proposed SM system allows a simple search over a small number of constellation pairs. In the simulation section, we compare the performance of the proposed scheme with other closed-loop systems such as the optimal unitary precoding (OUP) [16] and the optimal linear precoding (OLP) [8] over flat-fading quasi-static channels in terms of bit-error rate (BER).

The organization of the paper is as follows: Section II presents the system model and reviews conventional precoding schemes. In Section III, we propose a new SM scheme and show that the proposed transmission scheme attains single-symbol decodability at the receiver. Section IV illustrates the antenna-selection method based on the Euclidean distance between received vectors in the proposed SM system. In Section V, the simulation results are presented, comparing the proposed method with other precoding schemes. Finally, the paper ends with conclusions in Section VI.

## II. SYSTEM DESCRIPTIONS

In this section, we consider an SM system with  $M_t$  transmit and  $M_r$  receive antennas. We assume that the elements of the MIMO channel matrix are obtained from an independent and identically distributed (i.i.d.) complex Gaussian distribution. Each channel realization is assumed to be known at the receiver. Throughout this paper, normal letters represent scalar quantities, boldface letters indicate vectors, and boldface uppercase letters designate matrices. With a bar accounting for complex variables, for any complex notation  $\bar{c}$ , we denote the real and imaginary part of  $\bar{c}$  by  $\Re[\bar{c}]$  and  $\Im[\bar{c}]$ , respectively.

Let us define the  $M_t$ -dimensional complex transmitted signal vector  $\bar{\mathbf{x}}$ , and the  $M_r$ -dimensional complex received signal vector  $\bar{\mathbf{y}}$ . Then the complex received signal is given by

$$\bar{\mathbf{y}} = \bar{\mathbf{H}}\bar{\mathbf{x}} + \bar{\mathbf{n}} \quad (1)$$

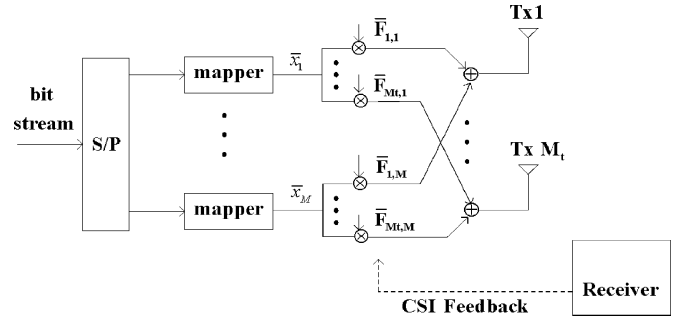


Fig. 1. Schematic diagram of transmission from  $M_t$  transmit antennas in closed-loop precoding MIMO systems.

where  $\bar{\mathbf{n}}$  is a complex Gaussian noise vector with covariance matrix  $\sigma_n^2 \mathbf{I}_{M_r}$ , and  $\mathbf{I}_d$  indicates an identity matrix of size  $d$ . Here the channel response matrix can be written as

$$\bar{\mathbf{H}} = \begin{bmatrix} \bar{H}_{11} & \cdots & \bar{h}_{1M_t} \\ \vdots & \ddots & \vdots \\ \bar{h}_{M_r1} & \cdots & \bar{h}_{M_rM_t} \end{bmatrix}$$

where  $\bar{h}_{ji}$  represents the channel response between the  $i$ th transmit and the  $j$ th receive antennas.

In what follows, we briefly review other two closed-loop schemes. The system consists of a spatial demultiplexer that produces  $M$  independent data streams, and a spatial precoder that maps these  $M$  streams to  $M_t$  transmit antennas ( $M \leq M_t$ ), as shown in Fig. 1. Here  $\bar{\mathbf{F}}$  denotes the  $M_t$  by  $M$  precoding matrix, and  $\bar{F}_{ij}$  indicates the  $(i, j)$  element of  $\bar{\mathbf{F}}$ . First, we consider the unitary precoding scheme proposed in [16] for limited feedback cases. Denoting  $\bar{\mathbf{U}}(m, n)$  as a set of  $m$  by  $n$  matrices with orthogonal columns, the SVD of  $\bar{\mathbf{H}}$  is given by

$$\bar{\mathbf{H}} = \bar{\mathbf{U}}\bar{\mathbf{\Sigma}}\bar{\mathbf{V}}^* \quad (2)$$

where  $\bar{\mathbf{U}} \in \bar{\mathbf{U}}(M_r, M_r)$ ,  $\bar{\mathbf{V}} \in \bar{\mathbf{U}}(M_t, M_t)$ , and  $\bar{\mathbf{\Sigma}}$  denotes an  $M_r$  by  $M_t$  diagonal matrix with the  $k$ th singular value of  $\bar{\mathbf{H}}$  at entry  $(k, k)$ . Here,  $*$  represents the complex conjugate transpose.

Then the optimal precoder  $\bar{\mathbf{F}}_{\text{opt}} \in \bar{\mathbf{U}}(M_t, M)$  is given by  $\bar{\mathbf{F}}_{\text{opt}} = \bar{\mathbf{V}}_M$  [16], where  $\bar{\mathbf{V}}_M$  is a matrix constructed from the first  $M$  columns of  $\bar{\mathbf{V}}$ . We refer to this precoder as *OUP*.

Second, for the case of full CSI at the transmitter, we consider the optimum linear precoder using the minimum mean-squared error (MMSE) criterion subject to a transmitted power constraint. Then the optimal linear precoder can be described by  $\bar{\mathbf{F}}_{\text{opt}} = \bar{\mathbf{V}}_M \bar{\mathbf{\Phi}}_f$  with the diagonal matrix  $\bar{\mathbf{\Phi}}_f$  given by [8]

$$\bar{\mathbf{\Phi}}_f = \left( \frac{\sigma_n}{\sqrt{E_s} \mu} \bar{\mathbf{\Sigma}}_M^{-1} - \frac{\sigma_n^2}{E_s} \bar{\mathbf{\Sigma}}_M^{-2} \right)_+^{1/2} \quad (3)$$

where  $(\cdot)_+$  indicates that negative elements of the matrix are replaced by zero,  $\mu$  is a parameter computed according to the total transmit power constraint, and  $\bar{\mathbf{\Sigma}}_M$  represents the  $M \times M$  upper-left matrix of the diagonal matrix  $\bar{\mathbf{\Sigma}}$ . We denote this precoder as *OLP*.

The main problem with these approaches in (2) and (3) is that the conventional precodings require high-complexity processing associated with SVD and high feedback overhead in sending information on the channel or precoding matrices. In the following sections, we propose a new SM scheme with reduced complexity and overhead.

### III. NEW SM SCHEME

In this section, we present an OSM scheme based on a single phase value, and show how to simplify the ML detection for the SM systems with two transmit antennas ( $M_t = 2$ ). As opposed to other limited-feedback schemes [17], [19] where sub-optimal receivers are employed, the proposed approach attains the optimal system performance by preserving the MLD at the receiver.

Let  $Q$  denote a signal constellation of size  $M_c$ . Given the channel matrix  $\bar{\mathbf{H}}$ , the ML estimate of the transmitted vector  $\bar{\mathbf{x}}$  is given by

$$\hat{\bar{\mathbf{x}}} = [\hat{x}_1 \ \hat{x}_2]^t = \arg \min_{\bar{\mathbf{x}} \in Q^2} \|\bar{\mathbf{y}} - \bar{\mathbf{H}}\bar{\mathbf{x}}\|^2 \quad (4)$$

where  $[\cdot]^t$  indicates the transpose of a vector or matrix and  $\|\cdot\|$  denotes the Euclidean norm. Note that the MLD complexity is exponential in the number of constellation points.

Equivalently, the real-valued representation of the system (1) can be written as [21]

$$\mathbf{y} = \begin{bmatrix} \Re[\bar{\mathbf{y}}] \\ \Im[\bar{\mathbf{y}}] \end{bmatrix} = \mathbf{H}\mathbf{x} + \mathbf{n} \quad (5)$$

where  $\mathbf{x} = [\Re[\bar{\mathbf{x}}^t] \ \Im[\bar{\mathbf{x}}^t]]^t$ ,  $\mathbf{n} = [\Re[\bar{\mathbf{n}}^t] \ \Im[\bar{\mathbf{n}}^t]]^t$ , and

$$\begin{aligned} \mathbf{H} &= \begin{bmatrix} \Re[\bar{\mathbf{H}}] & -\Im[\bar{\mathbf{H}}] \\ \Im[\bar{\mathbf{H}}] & \Re[\bar{\mathbf{H}}] \end{bmatrix} \\ &= \begin{bmatrix} \Re[\bar{h}_{11}] & \Re[\bar{h}_{12}] & -\Im[\bar{h}_{11}] & -\Im[\bar{h}_{12}] \\ \vdots & \vdots & \vdots & \vdots \\ \Re[\bar{h}_{M_r,1}] & \Re[\bar{h}_{M_r,2}] & -\Im[\bar{h}_{M_r,1}] & -\Im[\bar{h}_{M_r,2}] \\ \Im[\bar{h}_{11}] & \Im[\bar{h}_{12}] & \Re[\bar{h}_{11}] & \Re[\bar{h}_{12}] \\ \vdots & \vdots & \vdots & \vdots \\ \Im[\bar{h}_{M_r,1}] & \Im[\bar{h}_{M_r,2}] & \Re[\bar{h}_{M_r,1}] & \Re[\bar{h}_{M_r,2}] \end{bmatrix} \\ &= [\mathbf{h}_1 \ \mathbf{h}_2 \ \mathbf{h}_3 \ \mathbf{h}_4]. \end{aligned} \quad (6)$$

Here  $\mathbf{n}$  is a real Gaussian noise vector with covariance matrix  $(\sigma_n^2/2)\mathbf{I}_{2M_r}$ .

From the real-valued representation of the channel matrix in (6), it is easy to see that the column vectors  $\mathbf{h}_1$  and  $\mathbf{h}_2$  are orthogonal to  $\mathbf{h}_3$  and  $\mathbf{h}_4$ , respectively ( $\mathbf{h}_1 \perp \mathbf{h}_3$  and  $\mathbf{h}_2 \perp \mathbf{h}_4$ ). We also notice that  $\mathbf{h}_1 \cdot \mathbf{h}_2 = \mathbf{h}_3 \cdot \mathbf{h}_4$  and  $\mathbf{h}_1 \cdot \mathbf{h}_4 = -\mathbf{h}_2 \cdot \mathbf{h}_3$ , where  $\mathbf{h}_i \cdot \mathbf{h}_j$  denotes the inner (dot) product between vectors  $\mathbf{h}_i$  and  $\mathbf{h}_j$ . For the rest of this section, we will see that these properties are essential to the development of the new SM scheme.

Based on the real-valued representation in (5), the ML solution  $\hat{\bar{\mathbf{x}}}$  to (4) can be alternatively obtained by

$$\hat{\bar{\mathbf{x}}} = [\hat{x}_1 \ \hat{x}_2]^t = \arg \min_{\bar{\mathbf{x}} \in Q^2} \left\| \mathbf{y} - \mathbf{H} \begin{bmatrix} \Re[\bar{\mathbf{x}}] \\ \Im[\bar{\mathbf{x}}] \end{bmatrix} \right\|^2. \quad (7)$$

Note that the ML estimation metric (4) and (7) require the same amount of computation.

In what follows, we present the OSM to simplify the MLD. To achieve this goal, we encode the two transmitted symbols as

$$\mathcal{F}(\bar{\mathbf{x}}, \theta) = \begin{bmatrix} 1 & 0 \\ 0 & \exp(j\theta) \end{bmatrix} \mathbf{s}(\bar{\mathbf{x}}) \quad (8)$$

where  $\theta$  is the rotation phase angle applied to the second antenna and

$$\mathbf{s}(\bar{\mathbf{x}}) \triangleq \begin{bmatrix} \Re[\bar{x}_1] + j\Re[\bar{x}_2] \\ \Im[\bar{x}_1] + j\Im[\bar{x}_2] \end{bmatrix}.$$

With the above precoding, the original system model in (1) is transformed into

$$\bar{\mathbf{y}} = \bar{\mathbf{H}}\mathcal{F}(\bar{\mathbf{x}}, \theta) + \bar{\mathbf{n}} = \bar{\mathbf{H}}_\theta \mathbf{s}(\bar{\mathbf{x}}) + \bar{\mathbf{n}} \quad (9)$$

where

$$\bar{\mathbf{H}}_\theta = \bar{\mathbf{H}} \begin{bmatrix} 1 & 0 \\ 0 & \exp(j\theta) \end{bmatrix}.$$

Here  $\bar{\mathbf{H}}_\theta$  accounts for the effective channel matrix for  $\mathbf{s}(\bar{\mathbf{x}})$ .

Then, the real-valued system model corresponding to (9) can be represented as

$$\begin{aligned} \mathbf{y} &= \begin{bmatrix} \Re[\bar{\mathbf{y}}] \\ \Im[\bar{\mathbf{y}}] \end{bmatrix} = \begin{bmatrix} \Re[\bar{\mathbf{H}}_\theta] & -\Im[\bar{\mathbf{H}}_\theta] \\ \Im[\bar{\mathbf{H}}_\theta] & \Re[\bar{\mathbf{H}}_\theta] \end{bmatrix} \begin{bmatrix} \Re[\mathbf{s}(\bar{\mathbf{x}})] \\ \Im[\mathbf{s}(\bar{\mathbf{x}})] \end{bmatrix} + \begin{bmatrix} \Re[\bar{\mathbf{n}}] \\ \Im[\bar{\mathbf{n}}] \end{bmatrix} \\ &= [\mathbf{h}_1^\theta \ \mathbf{h}_2^\theta \ \mathbf{h}_3^\theta \ \mathbf{h}_4^\theta] \begin{bmatrix} \Re[\bar{x}_1] \\ \Im[\bar{x}_1] \\ \Re[\bar{x}_2] \\ \Im[\bar{x}_2] \end{bmatrix} + \mathbf{n} \end{aligned} \quad (10)$$

where the real column vector  $\mathbf{h}_i^\theta$  of length  $2M_r$  denotes the  $i$ th column of the effective real-valued channel matrix. Recall that the column vectors  $\mathbf{h}_1^\theta$  and  $\mathbf{h}_2^\theta$  are orthogonal to  $\mathbf{h}_3^\theta$  and  $\mathbf{h}_4^\theta$ , respectively, regardless of  $\theta$ . In this case, the SM scheme becomes fully orthogonal if and only if  $\mathbf{h}_1^\theta \perp \mathbf{h}_4^\theta$  and  $\mathbf{h}_2^\theta \perp \mathbf{h}_3^\theta$ . Note that both the channel capacity and the transmit power remain the same for the rotated channel for any  $\theta$ .

Denoting  $\bar{h}_{ij}^\theta$  as the  $(i, j)$ th entry of  $\bar{\mathbf{H}}_\theta$ , we obtain the inner product between  $\mathbf{h}_1^\theta$  and  $\mathbf{h}_4^\theta$  as

$$\begin{aligned} \mathbf{h}_1^\theta \cdot \mathbf{h}_4^\theta &= (\mathbf{h}_1^\theta)^t \mathbf{h}_4^\theta \\ &= -\sum_{m=1}^{M_r} \Re[\bar{h}_{m1}^\theta] \Im[\bar{h}_{m2}^\theta] + \sum_{m=1}^{M_r} \Im[\bar{h}_{m1}^\theta] \Re[\bar{h}_{m2}^\theta]. \end{aligned}$$

After some mathematical manipulations, this can be rewritten as

$$\begin{aligned} \mathbf{h}_1^\theta \cdot \mathbf{h}_4^\theta &= \cos \theta \sum_{m=1}^{M_r} |\bar{h}_{m1}| |\bar{h}_{m2}| \sin(\angle \bar{h}_{m1} - \angle \bar{h}_{m2}) \\ &\quad - \sin \theta \sum_{m=1}^{M_r} |\bar{h}_{m1}| |\bar{h}_{m2}| \cos(\angle \bar{h}_{m1} - \angle \bar{h}_{m2}) \end{aligned} \quad (11)$$

where  $|\cdot|$  and  $\angle$  indicate the magnitude and the phase of a complex number, respectively.

Since  $\mathbf{h}_2^\theta \cdot \mathbf{h}_3^\theta = -\mathbf{h}_1^\theta \cdot \mathbf{h}_4^\theta$ , the orthogonality of the SM can be achieved as long as (11) becomes zero. After trigonometric computations on (11), the rotation angle for the orthogonality between  $\mathbf{h}_1^\theta$  and  $\mathbf{h}_4^\theta$  (or  $\mathbf{h}_2^\theta$  and  $\mathbf{h}_3^\theta$ ) can be written as

$$\theta = \tan^{-1}\left(\frac{B}{A}\right) \pm \frac{\pi}{2} \quad (12)$$

where  $A = \sum_{m=1}^{M_r} |\bar{h}_{m1}| |\bar{h}_{m2}| \sin(\angle \bar{h}_{m2} - \angle \bar{h}_{m1})$  and  $B = \sum_{m=1}^{M_r} |\bar{h}_{m1}| |\bar{h}_{m2}| \cos(\angle \bar{h}_{m2} - \angle \bar{h}_{m1})$ .

Using the rotation angle of (12), we can achieve the orthogonality between transmitted signals in (10), where the subspace spanned by  $\mathbf{h}_1^\theta$  and  $\mathbf{h}_2^\theta$  becomes orthogonal to that spanned by  $\mathbf{h}_3^\theta$  and  $\mathbf{h}_4^\theta$ . As shown in [22], using this orthogonality, the ML solution  $\hat{\mathbf{x}} = [\hat{x}_1 \hat{x}_2]^t$  in (7) can be individually given by

$$\hat{x}_1 = \arg \min_{\bar{x} \in Q} \left\| \mathbf{y} - [\mathbf{h}_1^\theta \ \mathbf{h}_2^\theta] \begin{bmatrix} \Re[\bar{x}] \\ \Im[\bar{x}] \end{bmatrix} \right\|^2 \quad (13)$$

and

$$\hat{x}_2 = \arg \min_{\bar{x} \in Q} \left\| \mathbf{y} - [\mathbf{h}_3^\theta \ \mathbf{h}_4^\theta] \begin{bmatrix} \Re[\bar{x}] \\ \Im[\bar{x}] \end{bmatrix} \right\|^2. \quad (14)$$

Note that in determining  $\hat{x}_1$  and  $\hat{x}_2$  in (13) and (14), the size of the search set reduces to  $Q$ . These MLD equations show that with the proposed transmission scheme, the MLD at the receiver can be done by searching for a single symbol (called *single-symbol decodable*), while the traditional MLD in (4) requires searching a pair of symbols. Therefore, in our proposed SM system, the decoding complexity reduces from  $\mathcal{O}(M_c^2)$  to  $\mathcal{O}(M_c)$ , where the complexity accounts for the number of search candidates in the MLD.

As far as power allocation is concerned, the proposed OSM exhibits distinct characteristics compared with the SVD-based transmission schemes such as OUP and OLP. In the case of OUP, the channel gain associated with each subchannel is directly proportional to their singular values. This means that subchannels with small eigenmodes may be more prone to errors, compared with the other. In order to prevent this problem, the OLP scheme allocates more power to the weaker modes for an improved system performance. In contrast, in OSM, two transmitted symbols  $\bar{x}_1$  and  $\bar{x}_2$  in (10) experience effective channels with the same quality, since  $\|\mathbf{h}_1^\theta\| = \|\mathbf{h}_3^\theta\|$ ,  $\|\mathbf{h}_2^\theta\| = \|\mathbf{h}_4^\theta\|$ , and  $\mathbf{h}_1^\theta \cdot \mathbf{h}_2^\theta = \mathbf{h}_3^\theta \cdot \mathbf{h}_4^\theta$ . Consequently, there is no need for power allocation in the proposed OSM systems.

#### IV. ANTENNA-SELECTION SCHEME FOR OSM

In the previous section, we have presented a new SM scheme with two transmit antennas. Now we will extend the proposed scheme to systems with more than two transmit antennas. To this end, we introduce a simplified antenna-selection method for the proposed SM system. We first describe a criterion based on the minimum Euclidean distance between received vectors, and show that the proposed SM scheme substantially reduces the size of subsets to search for difference vectors, depending on the channel's geometrical properties.

We assume an SM system with  $M_t$  transmit antennas and  $M_r$  receive antennas where two independent eigenmodes are con-

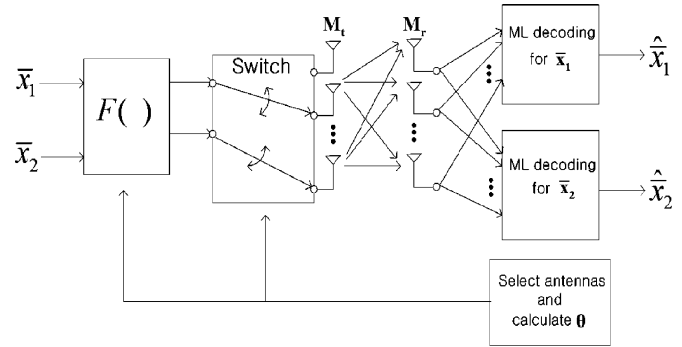


Fig. 2. Block diagram of a limited-feedback MIMO system.

sidered. The general data path for the proposed MIMO transmission is shown in Fig. 2. Two input symbols are precoded by the function  $\mathcal{F}(\bar{\mathbf{x}}, \theta)$  as in (8), and are transmitted over two transmit antennas out of  $M_t$  transmit antennas. The optimal selection of two transmit antennas is made based on the minimum Euclidean distance, since the Euclidean distance accounts for the performance of the ML receiver at high SNR [20].

Let  $\mathbf{P}(M_t, 2)$  denote the set of all possible  $\binom{M_t}{2} = (M_t(M_t - 1))/2$  subsets out of  $M_t$  transmit antennas. For a subset  $P \in \mathbf{P}(M_t, 2)$ , the receive constellation is defined as  $\{\bar{\mathbf{H}}_P^\theta(\bar{\mathbf{x}}) | \bar{\mathbf{x}} \in Q^2\}$  [20] where  $\bar{\mathbf{H}}_P^\theta$  denotes the  $M_r \times 2$  virtual channel matrix corresponding to the transmit antenna subset  $P$ . Then, we need to determine the optimum subset  $P$  whose squared minimum distance  $d_{\min}^2(P)$  between transmitted vectors  $\bar{\mathbf{x}}_c$  and  $\bar{\mathbf{x}}_e$  is the greatest. We compute  $d_{\min}^2(P)$  as

$$\begin{aligned} d_{\min}^2(P) &= \min_{\bar{\mathbf{x}}_c, \bar{\mathbf{x}}_e \in Q^2} \left\| \bar{\mathbf{H}}_P^\theta(\bar{\mathbf{x}}_c - \bar{\mathbf{x}}_e) \right\|^2 \\ &= \min_{\bar{\mathbf{x}}_c, \bar{\mathbf{x}}_e \in Q^2} \left\| [\mathbf{h}_{P,1}^\theta \ \mathbf{h}_{P,2}^\theta \ \mathbf{h}_{P,3}^\theta \ \mathbf{h}_{P,4}^\theta] \begin{bmatrix} \Re[\bar{x}_{1,c} - \bar{x}_{1,e}] \\ \Im[\bar{x}_{1,c} - \bar{x}_{1,e}] \\ \Re[\bar{x}_{2,c} - \bar{x}_{2,e}] \\ \Im[\bar{x}_{2,c} - \bar{x}_{2,e}] \end{bmatrix} \right\|^2 \end{aligned} \quad (15)$$

where  $\mathbf{h}_{P,i}^\theta$  is the  $i$ th column of the real-valued representation of  $\bar{\mathbf{H}}_P^\theta$ . Since the computation of  $d_{\min}^2(P)$  involves all possible pairs of  $\bar{\mathbf{x}}_c$  and  $\bar{\mathbf{x}}_e$ , the conventional SM systems require a search over  $\binom{M_c^2}{2} = (M_c^2(M_c^2 - 1))/2$  vectors.

In the following, we show that the proposed SM allows us to obtain the minimum distance in a much simpler form. Note that the subspace spanned by  $\mathbf{h}_{P,1}^\theta$  and  $\mathbf{h}_{P,2}^\theta$  is orthogonal to that spanned by  $\mathbf{h}_{P,3}^\theta$  and  $\mathbf{h}_{P,4}^\theta$ . In this case, assuming that two symbols  $\bar{x}_1$  and  $\bar{x}_2$  are independent of each other, (15) can be rewritten as

$$\begin{aligned} d_{\min}^2(P) &= \min_{\bar{x}_{1,c}, \bar{x}_{1,e} \in Q} \left\| [\mathbf{h}_{P,1}^\theta \ \mathbf{h}_{P,2}^\theta] \begin{bmatrix} \Re[\bar{x}_{1,c} - \bar{x}_{1,e}] \\ \Im[\bar{x}_{1,c} - \bar{x}_{1,e}] \end{bmatrix} \right\|^2 \\ &\quad + \min_{\bar{x}_{2,c}, \bar{x}_{2,e} \in Q} \left\| [\mathbf{h}_{P,3}^\theta \ \mathbf{h}_{P,4}^\theta] \begin{bmatrix} \Re[\bar{x}_{2,c} - \bar{x}_{2,e}] \\ \Im[\bar{x}_{2,c} - \bar{x}_{2,e}] \end{bmatrix} \right\|^2. \end{aligned} \quad (16)$$

Furthermore, we note that the first term on the right-hand side of (16) has the same minimum distance as the second term, since the geometrical relationship between  $\mathbf{h}_{P,1}^\theta$  and  $\mathbf{h}_{P,2}^\theta$  remains the

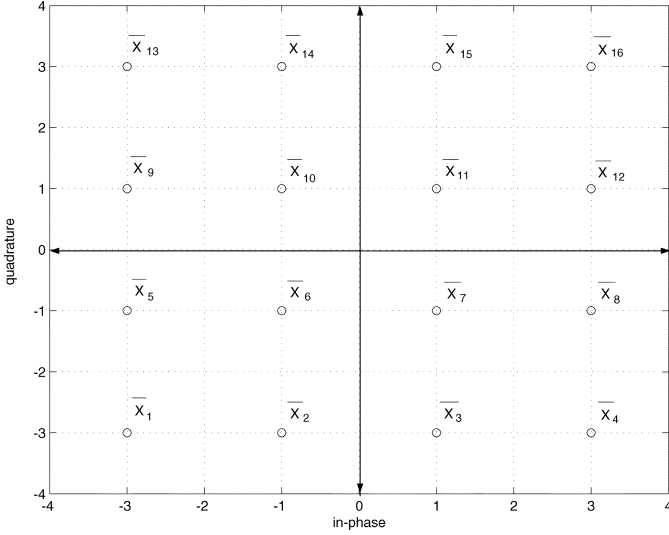


Fig. 3. 16 QAM constellation.

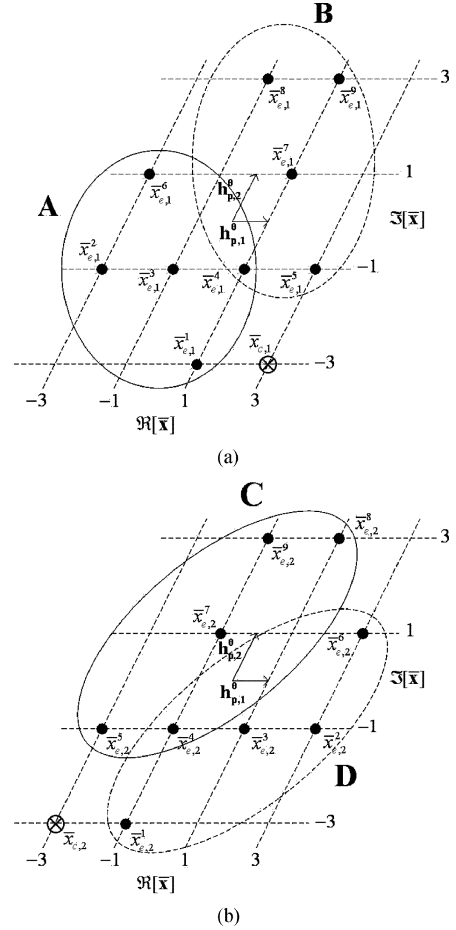
same as that between  $\mathbf{h}_{P,3}^\theta$  and  $\mathbf{h}_{P,4}^\theta$  (i.e.,  $\|\mathbf{h}_{P,1}^\theta\| = \|\mathbf{h}_{P,3}^\theta\|$ ,  $\|\mathbf{h}_{P,2}^\theta\| = \|\mathbf{h}_{P,4}^\theta\|$ , and  $\mathbf{h}_{P,1}^\theta \cdot \mathbf{h}_{P,2}^\theta = \mathbf{h}_{P,3}^\theta \cdot \mathbf{h}_{P,4}^\theta$ ). This symmetry means that, in the computation of the minimum distance, we need to consider only one of the two terms in (16) while assuming that the other term is zero. In other words, we can set  $\bar{x}_{2,c} = \bar{x}_{2,e}$  while  $d_{\min}^2(P)$  is computed with  $\bar{x}_{1,c} \neq \bar{x}_{1,e}$ . Let us define a difference vector as  $\mathbf{e}(\bar{x}_c, \bar{x}_e) = [\Re[\bar{x}_c - \bar{x}_e] \Im[\bar{x}_c - \bar{x}_e]]^t$  with  $\bar{x}_c \neq \bar{x}_e$ . Then, (16) can be simplified as

$$d_{\min}^2(P) = \min_{\bar{x}_c, \bar{x}_e \in Q} \left\| [\mathbf{h}_{P,1}^\theta \mathbf{h}_{P,2}^\theta] \mathbf{e}(\bar{x}_c, \bar{x}_e) \right\|^2. \quad (17)$$

It is clear that the computation of  $d_{\min}^2(P)$  in (17) requires a search over  $\binom{M_c}{2} = (M_c(M_c - 1))/2$  vectors.

Now we will illustrate a way to reduce the computational complexity even further. Considering the symmetries in uniform quadrature amplitude modulation (QAM) constellations, we can significantly reduce the set of difference vectors to search in (17). For illustrative purposes, we consider 16 QAM as shown in Fig. 3. Note that, among all possible  $\binom{16}{2} = 120$  difference vectors  $\mathbf{e}(\bar{x}_c, \bar{x}_e)$ , there exist many equal and collinear difference vectors. For example, pairs  $(\bar{x}_4, \bar{x}_6)$  and  $(\bar{x}_{12}, \bar{x}_{14})$  yield the same difference vectors ( $\mathbf{e}(\bar{x}_4, \bar{x}_6) = \mathbf{e}(\bar{x}_{12}, \bar{x}_{14})$ ), while pairs  $(\bar{x}_4, \bar{x}_{10})$  and  $(\bar{x}_4, \bar{x}_7)$  are related as collinear difference vectors ( $\mathbf{e}(\bar{x}_4, \bar{x}_{10}) = 2\mathbf{e}(\bar{x}_4, \bar{x}_7)$ ). Then, by excluding these equal and collinear difference vectors, there exist only 18 distinct difference vectors where  $\bar{x}_1$  and  $\bar{x}_4$  are set as the correct symbol  $\bar{x}_c$ . The corresponding pairs are illustrated as  $(\bar{x}_{c,i}, \bar{x}_{e,i}^k)$  for  $i \in \{1, 2\}$  and  $k \in \{1, 2, \dots, 9\}$  in Fig. 4. In this figure, the real and imaginary parts of the complex-valued symbols  $\bar{x}_{c,i}$  and  $\bar{x}_{e,i}^k \in \{\pm 3 \pm j3, \pm 3 \pm j1, \pm 1 \pm j3, \pm 1 \pm j1\}$  are displayed in real vector space with the basis vectors  $\mathbf{h}_{P,1}^\theta$  and  $\mathbf{h}_{P,2}^\theta$ , resulting in the tilted receive constellation. In this case, the distance from a point  $\bar{x}_{c,i}$  to a point  $\bar{x}_{e,i}^k$  in the figure corresponds to the Euclidean distance  $\|[\mathbf{h}_{P,1}^\theta \mathbf{h}_{P,2}^\theta] \mathbf{e}(\bar{x}_{c,i}, \bar{x}_{e,i}^k)\|$ .

Depending on the channel's geometrical properties such as the norm and the inner product of  $\mathbf{h}_{P,1}^\theta$  and  $\mathbf{h}_{P,2}^\theta$ , we can determine the set  $\hat{\chi}_{c-e}$  of  $\mathbf{e}(\bar{x}_c, \bar{x}_e)$  which is actually

Fig. 4. Reduced set of difference vectors in the receive constellation for  $\bar{\mathbf{h}}_p^\theta$ .

used in the computation of  $d_{\min}^2(P)$  without any performance degradation. There are four different cases that we need to consider for determining  $\hat{\chi}_{c-e}$ . Those four cases are listed in Table I. As an example, we consider the case of  $\mathbf{h}_{P,1}^\theta \cdot \mathbf{h}_{P,2}^\theta \geq 0$  (i.e., the angle between  $\mathbf{h}_{P,1}^\theta$  and  $\mathbf{h}_{P,2}^\theta$  is less than or equal to  $\pi/2$ ) and  $\|\mathbf{h}_{P,1}^\theta\| \leq \|\mathbf{h}_{P,2}^\theta\|$ , which makes the receive constellation look like the one depicted in Fig. 4. It is clear in this figure that the first condition  $\mathbf{h}_{P,1}^\theta \cdot \mathbf{h}_{P,2}^\theta \geq 0$  guarantees  $\|[\mathbf{h}_{P,1}^\theta \mathbf{h}_{P,2}^\theta] \mathbf{e}(\bar{x}_{c,1}, \bar{x}_{e,1}^k)\| \leq \|[\mathbf{h}_{P,1}^\theta \mathbf{h}_{P,2}^\theta] \mathbf{e}(\bar{x}_{c,2}, \bar{x}_{e,2}^k)\|$  for any  $k$ . In this case, we only need to consider nine pairs of  $(\bar{x}_{c,1}, \bar{x}_{e,1}^k)$  in Fig. 4(a). Meanwhile, the latter condition  $\|\mathbf{h}_{P,1}^\theta\| \leq \|\mathbf{h}_{P,2}^\theta\|$  promises that  $\|[\mathbf{h}_{P,1}^\theta \mathbf{h}_{P,2}^\theta] \mathbf{e}(\bar{x}_{c,1}, \bar{x}_{e,1}^k)\| \leq \|[\mathbf{h}_{P,1}^\theta \mathbf{h}_{P,2}^\theta] \mathbf{e}(\bar{x}_{c,1}, \bar{x}_{e,1}^k)\|$  for  $(k_1, k_2) \in \{(1, 5), (2, 9), (3, 7), (6, 8)\}$ , since the points in the lower left part in Fig. 4(a) are closer to  $\bar{x}_{c,1}$  than those in the upper right part. As a result, under these two conditions,  $d_{\min}^2(P)$  can be obtained by searching only five pairs of  $(\bar{x}_{c,1}, \bar{x}_{e,1}^k)$  within Circle A in Fig. 4(a). We can generalize the candidate pairs  $(\bar{x}_c, \bar{x}_e)$  for the set  $\hat{\chi}_{c-e}$  as listed in Table I.

Finally,  $d_{\min}^2(P)$  can be expressed as

$$d_{\min}^2(P) = \min_{\mathbf{e}(\bar{x}_c, \bar{x}_e) \in \hat{\chi}_{c-e}} \left\| [\mathbf{h}_{P,1}^\theta \mathbf{h}_{P,2}^\theta] \mathbf{e}(\bar{x}_c, \bar{x}_e) \right\|^2 \quad (18)$$

which facilitates a search for the optimal antenna subset  $P^*$ .

TABLE I  
CANDIDATE PAIRS OF  $(\bar{x}_c, \bar{x}_e)$  FOR THE SET  $\hat{\mathcal{X}}_{c-e}$  OF  $e(\bar{x}_c, \bar{x}_e)$

Case	Mod	$(\Re[\bar{x}_c], \Im[\bar{x}_c])$	$(\Re[\bar{x}_e], \Im[\bar{x}_e])$
$\mathbf{h}_{P,1}^\theta \cdot \mathbf{h}_{P,2}^\theta \geq 0,$ $\ \mathbf{h}_{P,1}^\theta\  \leq \ \mathbf{h}_{P,2}^\theta\ $	QPSK	(1, -1)	(-1, ±1)
	16QAM	(3, -3)	(-3, ±1), (±1, -1), (1, -3) (points within Circle A in Fig. 4)
	64QAM	(7, -7)	(-7, ±5), (-7, ±3), (-7, ±1), (5, -7), (±5, -5), (-5, 3), (±3, -5), (-3, -3), (-3, ±1), (±1, -5), (1, -3), (-1, -1)
$\mathbf{h}_{P,1}^\theta \cdot \mathbf{h}_{P,2}^\theta \geq 0,$ $\ \mathbf{h}_{P,1}^\theta\  > \ \mathbf{h}_{P,2}^\theta\ $	QPSK	(1, -1)	(±1, 1)
	16QAM	(3, -3)	(±1, 3), (1, ±1), (3, -1) (points within Circle B in Fig. 4)
	64QAM	(7, -7)	(7, -5), (±5, 7), (5, ±5), (5, ±3), (5, ±1), (±3, 7), (-3, 5), (3, 3), (3, -1), (±1, 7), (±1, 3), (1, 1)
$\mathbf{h}_{P,1}^\theta \cdot \mathbf{h}_{P,2}^\theta < 0,$ $\ \mathbf{h}_{P,1}^\theta\  > \ \mathbf{h}_{P,2}^\theta\ $	QPSK	(-1, -1)	(±1, 1)
	16QAM	(-3, -3)	(±1, 3), (-1, ±1), (-3, -1) (points within Circle C in Fig. 4)
	64QAM	(-7, -7)	(-7, -5), (±5, 7), (-5, ±5), (-5, ±3), (-5, ±1), (±3, 7), (-3, 3), (-3, -1), (3, 5), (±1, 7), (±1, 3), (-1, 1)
$\mathbf{h}_{P,1}^\theta \cdot \mathbf{h}_{P,2}^\theta < 0,$ $\ \mathbf{h}_{P,1}^\theta\  \leq \ \mathbf{h}_{P,2}^\theta\ $	QPSK	(-1, -1)	(1, ±1)
	16QAM	(-3, -3)	(3, ±1), (±1, -1), (-1, -3) (points within Circle D in Fig. 4)
	64QAM	(-7, -7)	(7, ±5), (7, ±3), (7, ±1), (-5, -7), (±5, -5), (5, 3), (±3, -5), (3, -3), (3, ±1), (±1, -5), (-1, -3), (1, -1)

As a consequence, the optimal subset  $P^*$  from the entire set  $\mathbf{P}(M_t, 2)$  is obtained as

$$P^* = \arg \max_{P \in \mathbf{P}(M_t, 2)} d_{\min}^2(P).$$

It is important to note that the proposed SM scheme reduces the size of the set of candidate vectors in computing  $d_{\min}^2(P)$  from 120, 32 640, and 8 386 560 to 2, 5, and 19 for QPSK, 16 QAM, and 64 QAM, respectively, as (15) for the minimum Euclidean distance is equivalent to (18). Therefore, it is evident that the computational savings in the proposed scheme are substantial.

### V. SIMULATION RESULTS

In this section, we provide simulation results that illustrate the performance of our proposed OSM compared with the closed-loop schemes OUP and OLP. The number of transmitted data streams is fixed to two in all simulations, and the optimal transmit-antenna subset is chosen based on the minimum Euclidean distance in the OSM systems, as described in the previous section. It is clear that for the proposed OSM systems with more than two transmit antennas ( $M_t > 2$ ),  $\log_2 \binom{M_t}{2}$  bits are required to be sent back to the transmitter to determine the optimum antenna subset, which is the case with the conventional transmit-antenna selection. For a fair comparison, we assume an ML receiver for all systems.

In the first simulations, we demonstrate the proposed MLD method by evaluating the BER performance of OSM systems.

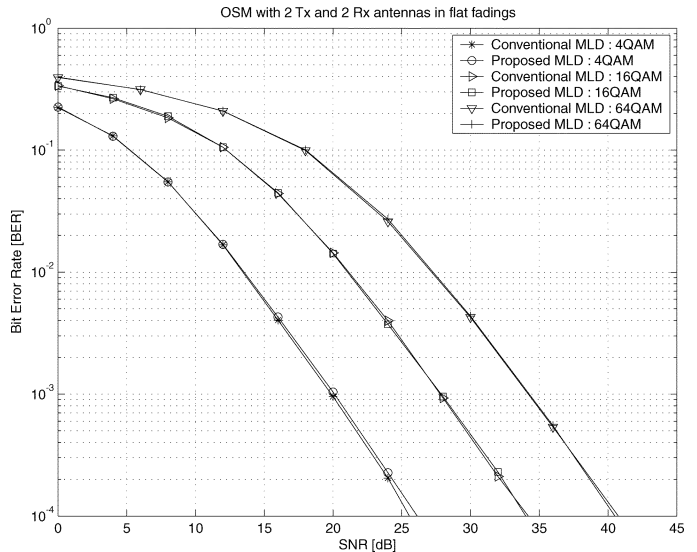


Fig. 5. BER performance for the proposed MLD and the conventional MLD.

In Fig. 5, the performance of our proposed MLD using (13) and (14) is compared with the performance of the conventional MLD given by (4) or (7). In this plot, we consider a MIMO system with two transmit and two receive antennas. This figure shows that the proposed MLD method provides the identical performance as the conventional MLD, yet the complexity of the new method is significantly lower.

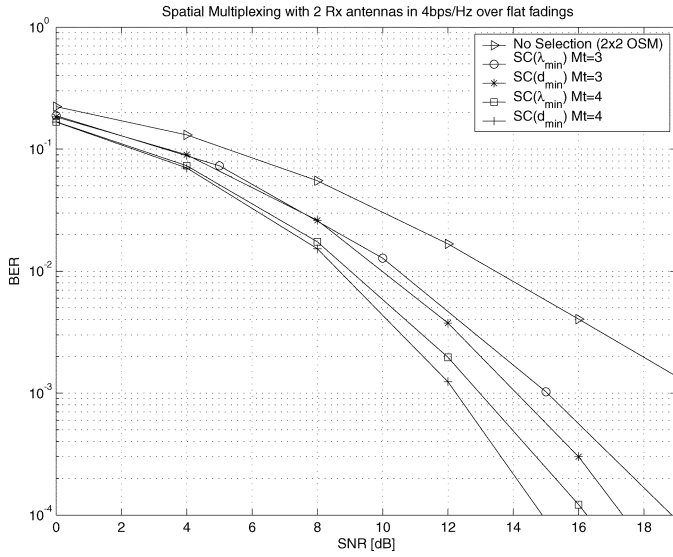


Fig. 6. BER performance comparison of different antenna-selection criteria.

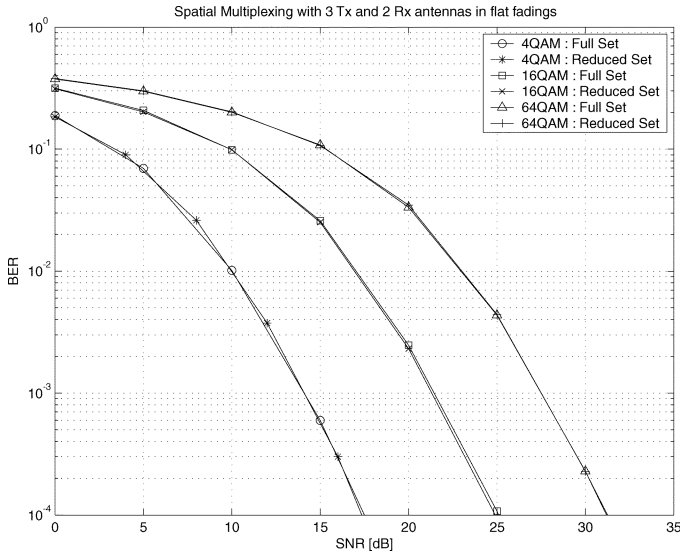
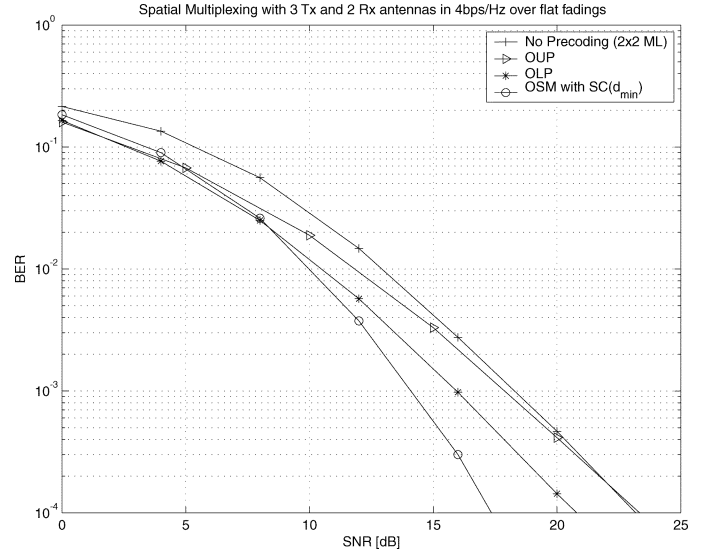
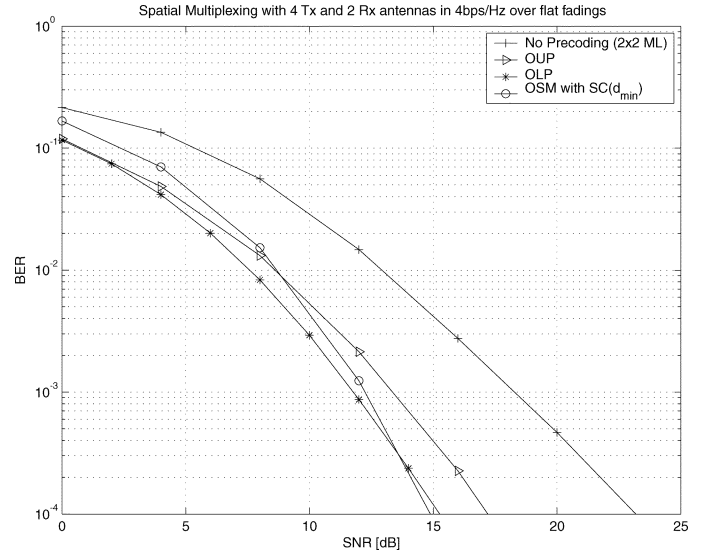


Fig. 7. BER performance comparison with the full and reduced sets of difference vectors.

Fig. 6 provides the performance comparison between different antenna-selection criteria for the proposed SM systems: the minimum Euclidean distance-based criterion (denoted by  $SC(d_{\min})$ ) and the minimum singular value-based criterion proposed in [17] (denoted by  $SC(\lambda_{\min})$ ). In this simulation, three or four transmit antennas and two receive antennas are considered with 4 QAM. Note that the selection criterion  $SC(\lambda_{\min})$  is originally designed for linear receivers instead of ML receivers. In contrast, the minimum eigenvalue  $\lambda_{\min}$  provides a lower bound for the minimum distance criterion [9]. As expected, the OSM system using  $SC(d_{\min})$  performs 1.3 dB better than  $SC(\lambda_{\min})$  at a BER of  $10^{-4}$ . Thus, from now on, we consider the selection criterion  $SC(d_{\min})$  for the proposed OSM system.

Next, in Fig. 7, we present the simulation results to demonstrate the efficacy of the simplified antenna-selection method introduced in Section IV. In this plot, we assume  $M_t = 3$  and  $M_r = 2$ . These simulation results reflect that the proposed antenna-selection method using (18) with the reduced set of differ-

Fig. 8. BER performance comparison of the SM schemes with  $M_t = 3$ .Fig. 9. BER performance comparison of the SM schemes with  $M_t = 4$ .

ence vectors provides performance identical to conventional antenna selection using (15) with the full set of difference vectors.

In Figs. 8 and 9, we depict the BER comparison of the OSM and two optimal precodings OUP and OLP with  $M_r = 2$  and 4 QAM. For comparison purposes, we also plot the performance of the  $2 \times 2$  SM with MLD at the receiver, where the number of the search candidates for the MLD is  $M_c^2$  without any precoding. For the  $M_t = 3$  case presented in Fig. 8, we can see that the OSM provides a 4 dB gain at a BER of  $10^{-3}$  over the no-precoding case. More importantly, Fig. 8 shows that the OSM outperforms both the OUP and OLP cases by 1.8 and 3.8 dB, respectively. As the number of transmit antennas increases to four as in Fig. 9, the selection gain of the OSM grows up to 7 dB compared with the  $2 \times 2$  ML case. The benefit of increasing the number of transmit antennas is more pronounced for OUP and OLP, since these precodings exploit available MIMO spatial diversity gains better than the simple SM. Nonetheless, the OSM performs within 0.5 dB of the OLP, and still outperforms the OUP by approximately 1 dB at a BER of  $10^{-3}$ . It should

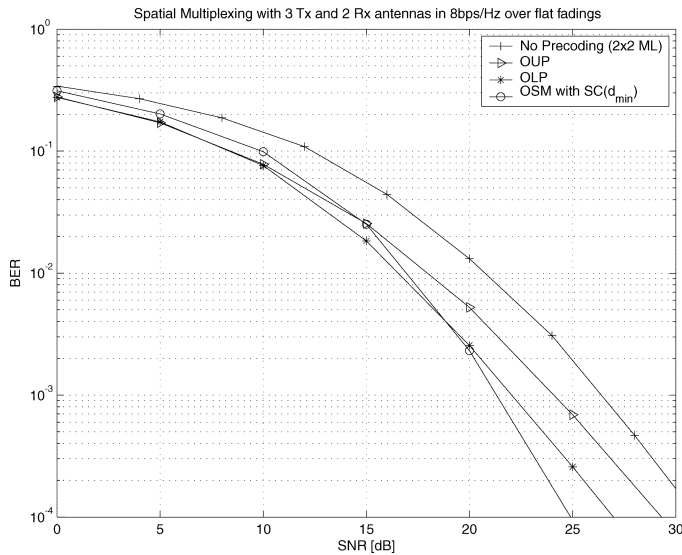


Fig. 10. BER performance comparison of the SM schemes with 16 QAM.

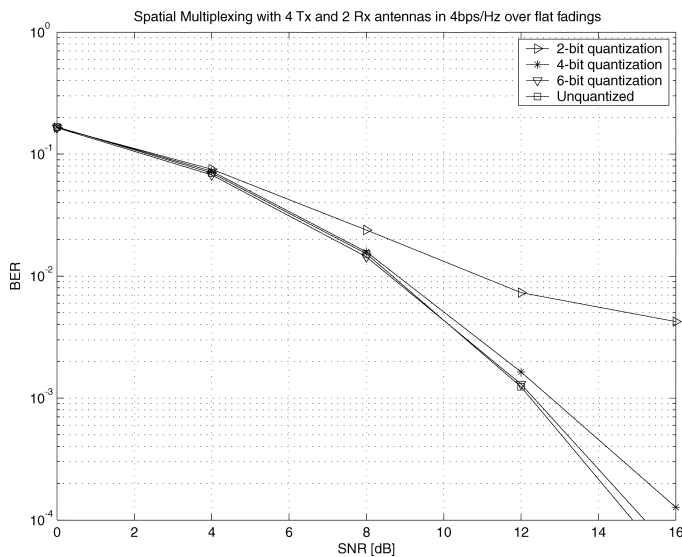


Fig. 11. Effect of quantization on BER performance.

be noted that in the conventional precoding systems we need to solve (2) and (3) to derive the precoding matrix by computing the SVD operation and the power-allocation matrix that determines the power distribution among the spatial modes. Moreover, these linear precodings involve complex-valued matrix-matrix and/or matrix-vector multiplications at the transmitter. Thus, the computation complexities of OLP and OUP are substantially higher than the proposed OSM. As for the feedback overhead, our proposed scheme needs only a single phase-value feedback, while the conventional precoding schemes require much larger feedback information in sending back the entire channel or precoding matrix, especially including the power-allocation matrix for the OLP.

Fig. 10 depicts the performance comparison for 16 QAM constellation with  $M_t = 3$  and  $M_r = 2$ . As observed in this figure, the proposed OSM outperforms the OLP by about 2 dB in the high-SNR regime with much-reduced complexity and overhead.

Finally, in Fig. 11, we illustrate the BER performance of the proposed OSM with respect to the number of quantized bits for

the phase value to evaluate the effect of quantization on the OSM performance. In a practical scenario, a smaller number of quantization bits are preferred to reduce the feedback amount. In this plot, four transmit antennas and two receive antennas are assumed with 4 QAM. This simulation shows that 6-bit quantized phase feedback is sufficient for the OSM schemes.

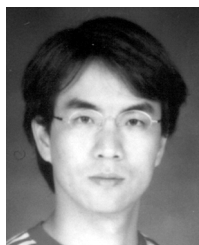
## VI. CONCLUSION

In this paper, we presented a new OSM scheme for MIMO systems which minimizes the overall complexity. The primary goal of this work is to maximize the system performance with a low complexity at the receiver while maintaining the optimal MLD. By taking a single phase-value feedback, simple orthogonal MLD is achieved. Also, we studied a criterion to choose the subset of transmit antennas that maximizes the minimum Euclidean distance of the receive constellation in the proposed SM system. Motivated by the fact that the computation of the minimum Euclidean distance requires a search over multidimensional constellations, we substantially reduce the candidate search size of difference vectors in the proposed SM system and present the reduced set of difference vectors for each constellation. The simulation results confirm that the proposed OSM scheme is quite effective in approaching the performance of the OLP with significantly reduced complexity and feedback amounts.

## REFERENCES

- [1] G. J. Foschini, "Layered space-time architecture for wireless communication in a fading environment when using multi-element antennas," *Bell Labs. Tech. J.*, vol. 1, pp. 41–59, 1996.
- [2] H. Lee and I. Lee, "New approach for error compensation in coded V-BLAST OFDM systems," *IEEE Trans. Commun.*, vol. 55, no. 2, pp. 345–355, Feb. 2007.
- [3] H. Lee, B. Lee, and I. Lee, "Iterative detection and decoding with an improved V-BLAST for MIMO-OFDM systems," *IEEE J. Sel. Areas Commun.*, vol. 24, no. 3, pp. 504–513, Mar. 2006.
- [4] G. J. Foschini and M. Gans, "On limits of wireless communications in a fading environment when using multiple antennas," *Wireless Pers. Commun.*, vol. 6, pp. 311–335, Mar. 1998.
- [5] I. E. Telatar, "Capacity of multi-antenna Gaussian channels," *Eur. Trans. Telecommun.*, vol. 10, pp. 585–595, Nov. 1999.
- [6] G. G. Raleigh and J. M. Cioffi, "Spatio-temporal coding for wireless communication," *IEEE Trans. Commun.*, vol. 46, no. 3, pp. 357–366, Mar. 1998.
- [7] J. B. Andersen, "Array gain and capacity for known random channels with multiple element arrays at both ends," *IEEE J. Sel. Areas Commun.*, vol. 18, no. 8, pp. 2172–2178, Nov. 2000.
- [8] H. Sampath, P. Stoica, and A. Paulraj, "Generalized linear precoder and decoder design for MIMO channels using the weighted MMSE criterion," *IEEE Trans. Commun.*, vol. 49, no. 12, pp. 2198–2206, Dec. 2001.
- [9] A. Scaglione, P. Stoica, S. Barbarossa, G. B. Giannakis, and H. Sampath, "Optimal designs for space-time linear precoders and decoders," *IEEE Trans. Signal Process.*, vol. 50, no. 5, pp. 1051–1064, May 2002.
- [10] A. J. Goldsmith, S. A. Jafar, N. J. Jindal, and S. Vishwanath, "Capacity limits of MIMO channels," *IEEE J. Sel. Areas Commun.*, vol. 21, no. 6, pp. 684–702, Jun. 2003.
- [11] E. Visotsky and U. Madhow, "Space-time transmit precoding with imperfect feedback," *IEEE Trans. Inf. Theory*, vol. 47, no. 9, pp. 2632–2639, Sep. 2001.
- [12] A. Narula, M. J. Lopez, M. D. Trott, and G. W. Wornell, "Efficient use of side information in multiple-antenna data transmission over fading channels," *IEEE J. Sel. Areas Commun.*, vol. 16, no. 7, pp. 1423–1436, Oct. 1998.
- [13] D. J. Love and R. W. Heath, "What is the value of limited feedback for MIMO channels," *IEEE Commun. Mag.*, vol. 42, pp. 54–59, Oct. 2004.
- [14] G. H. Golub and C. F. V. Loan, *Matrix Computations*, 2nd ed. Baltimore, MD: The Johns Hopkins Univ. Press, 1989.

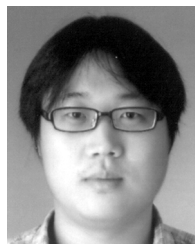
- [15] D. J. Love and R. W. Heath, "Limited feedback unitary precoding for orthogonal space-time block codes," *IEEE Trans. Signal Process.*, vol. 53, no. 1, pp. 64–73, Jan. 2005.
- [16] D. J. Love and R. W. Heath, "Limited feedback unitary precoding for spatial multiplexing systems," *IEEE Trans. Inf. Theory*, vol. 51, no. 8, pp. 2967–2976, Aug. 2005.
- [17] R. W. Heath, S. Sandhu, and A. J. Paulraj, "Antenna selection for spatial multiplexing systems with linear receivers," *IEEE Commun. Lett.*, vol. 5, no. 4, pp. 142–144, Apr. 2001.
- [18] D. A. Gore, R. U. Nabar, and A. J. Paulraj, "Selecting an optimal set of transmit antennas for a low-rank matrix channel," in *Proc. ICASSP*, Jun. 2000, vol. 5, pp. 2785–2788.
- [19] D. A. Gore, R. W. Heath, and A. J. Paulraj, "Transmit selection in spatial multiplexing systems," *IEEE Commun. Lett.*, vol. 6, no. 11, pp. 491–493, Nov. 2002.
- [20] R. W. Heath and A. J. Paulraj, "Antenna selection for spatial multiplexing systems based on minimum error rate," in *Proc. ICC*, Jun. 2001, vol. 7, pp. 2276–2280.
- [21] A. M. Chan and I. Lee, "A new reduced-complexity sphere decoder for multiple antenna systems," in *Proc. ICC*, Apr. 2002, pp. 460–464.
- [22] H. Lee, J. Cho, J.-K. Kim, and I. Lee, "An efficient decoding algorithm for STBC with multi-dimensional rotated constellations," in *Proc. ICC*, Jun. 2006, vol. 12, pp. 5558–5563.



**Heunchul Lee** (S'04) received the B.S. degree in electrical engineering in 2003 and the M.S. degree in radio communications engineering in 2005, both from Korea University, Seoul, Korea, where he is currently working toward the Ph.D. degree in the School of Electrical Engineering.

His research interests include space-time coding, signal processing, and coding for wireless communications, with current emphasis on signal processing techniques for MIMO-OFDM systems.

Mr. Lee received the Best Paper Award at the 12th Asia-Pacific Conference on Communications, and the IEEE Seoul Section Student Paper Contest award, both in 2006.



award, both in 2006.

**Seokhwan Park** (S'05) received the B.S. degree in electrical engineering in 2005 and the M.S. degree in radio communications engineering in 2007, both from Korea University, Seoul, Korea, where he is currently working toward the Ph.D. degree in the School of Electrical Engineering.

His research interests include signal processing techniques for MIMO-OFDM systems.

Mr. Park received the Best Paper Award at the 12th Asia-Pacific Conference on Communications, and the IEEE Seoul Section Student Paper Contest



**Inkyu Lee** (S'92–M'95–SM'01) was born in Seoul, Korea, in 1967. He received the B.S. degree (Hon.) in control and instrumentation engineering from Seoul National University, Seoul, Korea, in 1990, and the M.S. and Ph.D. degrees in electrical engineering from Stanford University, Stanford, CA, in 1992 and 1995, respectively.

From 1991 to 1995, he was a Research Assistant at the Information Systems Laboratory, Stanford University. From 1995 to 2001, he was a Member of Technical Staff at Bell Laboratories, Lucent

Technologies, where he studied the high-speed wireless system design. He later worked for Agere Systems (formerly Microelectronics Group of Lucent Technologies), Murray Hill, NJ, as a Distinguished Member of Technical Staff from 2001 to 2002. In September 2002, he joined the faculty of Korea University, Seoul, Korea, where he is currently an Associate Professor in the School of Electrical Engineering. He has published over 30 journal papers in IEEE, and has 20 U.S. patents granted or pending. His research interests include digital communications, signal processing, and coding techniques applied to wireless systems with an emphasis on MIMO-OFDM.

Dr. Lee currently serves as an Associate Editor for the IEEE TRANSACTIONS ON COMMUNICATIONS in the area of Wireless Communication Theory, and has also been a Guest Editor for the IEEE JOURNAL ON SELECTED AREAS IN COMMUNICATIONS (Special Issue on 4G Wireless Systems). He received the IT Young Engineer Award as the IEEE/IEEK joint award in 2006. Also in 2006, he received the APCC Best Paper Award.